Malkin, R., & Robert, D. (2014). High sensitivity non-contact method for dynamic quantification of elastic waves & strains in transparent media. Measurment, 55, 51-57. 10.1016/j.measurement.2014.04.038

High sensitivity non-contact method for dynamic quantification of elastic waves & strains in transparent media

Short title: Quantification of elastic waves in solid media

Robert Malkin*, Daniel Robert

Faculty of Science
University of Bristol, England, BS8 1TQ

Tel: +44 (0) 117 928 7484

*corresponding author: r.e.malkin@gmail.com

1 Abstract

This paper presents time resolved quantitative evaluation of elastic stress waves in solid media by utilising an adaptation of the well-established laser Doppler vibrometry method. We show that the introduction of elastic stress waves in a transparent medium gives rise to detectable and quantifiable changes in the refractive index, which is proportional to stress. The method is tested for mechanical excitation at frequencies from 10 to 25kHz in an acrylic bar. This refractometric quantification can measure internal strains as low as $1x10^{-11}$. Additionally, finite element analysis is conducted to gauge the validity of the results. In the presented work an acrylic bar is used, this method however should be applicable to any transparent solid.

Keywords:
1. Laser Doppler vibrometry
2. Refracto-vibrometry
3. Stress waves
4. Refractive index

2 Introduction

Photo-elasticity and Schlieren photography are two popular methods to visualise elastic waves in a solid. While photo-elasticity allows single transient events to be visualised, the quantification of stresses within the solid are time-consuming and especially challenging for 3D media [1]. Schlieren photography allows for high fidelity visualisation of stress fields in solids, it does not however readily allow for quantification [2]. Other methods such as neutron-diffraction [3], have also been used to quantify internal stresses, however the facilities required are highly specialised, whereas the present method requires a relatively inexpensive laser vibrometer. Earlier work by *Mattei et al.* [4] and *Jia et al* [5] demonstrated a similar refractometry based method to the one presented here, and were able to measure strains in acrylic with good agreement between experimental and analytical predictions. The method employed did however rely on an extensive mathematical treatment, perhaps excluding a large section of the non-specialist potential users. The method has also been used to accurately measure mechanical properties of solids [6]. The methods described in this paper allows for simple and rapid measurements of internal stress fields and are especially suitable to a non-specialist in acoustics/mechanics.

3 Theoretical background

The refractive index, n, of a medium is defined as;

$$n \equiv \frac{c_0}{v} \tag{1}$$

With c_0: velocity of light in a vacuum and v: the velocity of light in the medium. The refractive index of a medium is influenced by stress, density and temperature of the host medium [7][8]. If we consider a simple adiabatic (no change in system temperature), isochoric (no change in system volume) event in a solid domain where there is a change in stress, this will result in a corresponding change in n. Solids will exhibit either a positive or negative linear relationship between n and stress [8][9][10]. Monitoring the change in n (refractometry) can therefore be used to monitor stresses within solids. Probing dynamic events with traditional refractometry where n changes at frequencies in the kHz range is, as yet, not possible. What can be probed however, using Laser Doppler interferometry, is the variation in velocity, v, of light in the medium and therefore allowing stress to be estimated. The principle of the measurement technique is elegantly described by *Nakamura et al.* [11] and is reported here in Figure 1.

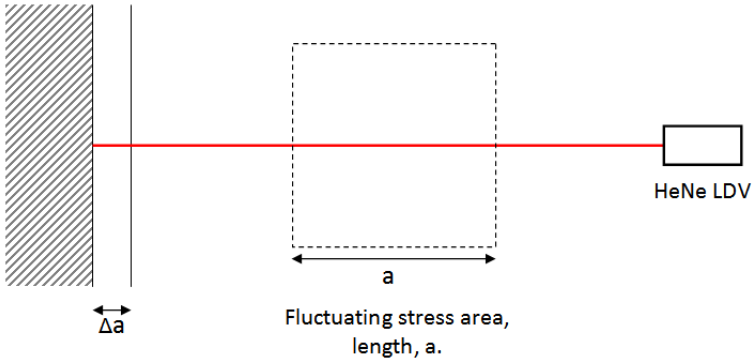

Figure 1 - Principle of measurement. The change in optical path length appears as a displacement of the rigid wall on the left. Adapted from [11]**.**

Monochromatic laser light is directed through a region of the medium, of length *a*, in which the stress fluctuates. The laser exits the region and if reflected from a rigid wall, back through the region and into the interferometer. This modulated path length, Δa, appears identical to a physical displacement of the reflective rigid wall.

$$\Delta n \cdot a = n \cdot \Delta a \tag{2}$$

The output signal from a laser Doppler vibrometer (LDV) is the velocity of the apparent displacement of the rigid wall, as shown in [12].

$$\Delta n = \frac{n}{a} \frac{v_{LDV}}{2 \cdot \pi \cdot f} \tag{3}$$

Where *f:* frequency of stress fluctuation and, v_{LDV}: velocity from LDV, which is integrated with respect to time to give the apparent displacement, Δa, as shown in Eq 2. Most refracto-vibrometry is primarily based on using the method for either air or water pressure measurement [13–17], with some preliminary work conducted into stresses in solids by *Zipser et. al*. [18]. The principle of measurement however holds for any medium, not just air. Therefore we developed an experimental procedure that enables the quantitative investigation of elastic waves propagating in a solid.
An empirical relation between the longitudinal strain, ε, of a block of polymethyl methacrylate (PMMA), and *n*, from Nazarov *et al* [10], is shown to be;

$$\frac{\Delta n}{\Delta \varepsilon} = 0.462 \; per \; Pa \tag{4}$$

Assuming that the elastic waves are within the linear elastic region, Eq 3 & 4 can be combined to generate an approximation of the stress, σ;

$$\Delta \sigma = E \cdot \Delta \varepsilon = \frac{n}{a} \frac{E}{0.462} \cdot \Delta a \tag{5}$$

Where *E*: Young's modulus and Δa the displacement from the integrated LDV velocity signal. Eq 5 shows that the stress/strain within the sample is directly related to the apparent displacement, Δa. Thus, the sensitivity of the method is determined by the sensitivity of the vibrometer. It should be noted that as the laser beam passes through a medium, its change in velocity will be averaged over the path length. Thus, the laser beam passing through a length of positive stress and then an equal

magnitude and length negative stress area would register a net stress change of zero. The presented application of the method only applies where the stress/strain magnitude is of equal magnitude along the laser path length. Therefore care needs to be taken to interpret any stress values calculated using the method. This 'line integration' issue is discussed in detail in [19], [20] and may be essentially eliminated when performing computer tomography, as shown by Olsson & Forsberg [14].

4 Experimental Methodology

Given the large amount of literature on the physical properties of PMMA, it was chosen as the experimental solid. A suitable method of producing an elastic wave was found to be the use of a piezo transducer (Maplin electronics YU-87U, ⌀25mm) attached to one end of the solid PMMA bar. An extruded PMMA square bar (20 x 20 x 500mm) was simply supported on top of two machined metal posts, supporting the span of the bar, as shown in Figure 2. The transducer (bonded to one end of the bar) was connected to a waveform generator (Agilent 33120A) and the voltage amplitude set such that the observed displacement of the transducer was constant between tested frequencies. A 5 cycle burst at a range of frequencies (10-25kHz) was periodically sent to the transducer. The cyclic burst waveform would allow us to perform a scan of the bar and thus allow the time evolution of the elastic waves to be observed using a scanning vibrometer (Polytec PSV-400).

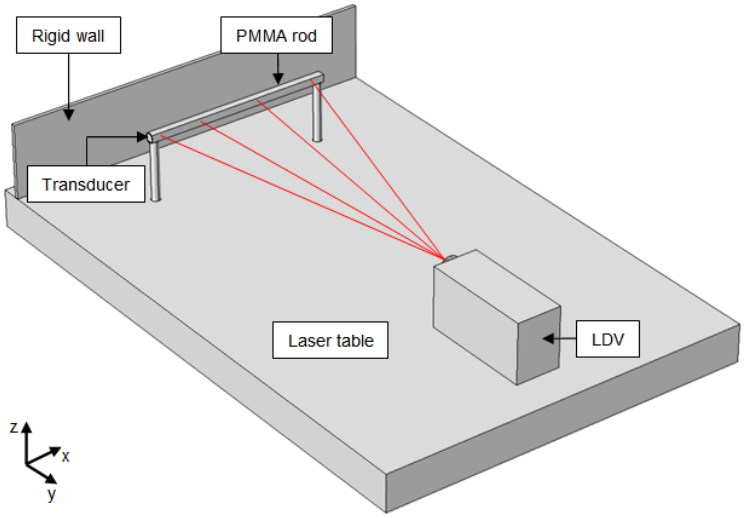

Figure 2 - Experimental set-up for observing stress changes in transparent solid.

For this experimental work, we observed two elastic wave types; longitudinal compression and Rayleigh surface waves. The question now arises as to how to separate these two waves from the LDV measurements.

It was observed that when focusing the laser beam on the surface of the highly transparent bar and removing the rigid reflector, Rayleigh surface waves could not be detected. This is attributed to insufficient light returning to the LDV. Rayleigh waves could only be observed by painting the surface parallel and closest to the LDV with a light coat of white spray paint (Figure 3-A). This

increased light reflection sufficiently to allow the surface waves to be observed. Because the PMMA bar exhibits only a single opaque reflective surface, only surface waves could contribute to the LDV measurement.

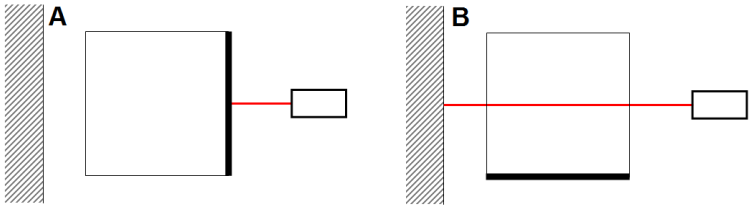

Figure 3 - Illustration of measurement technique. For A: Rayleigh surface wave, B: longitudinal. Thick black line indicates white paint on surface.

When measuring through the bar (Figure 3-B), it was assumed that only the longitudinal waves contributed to the observed stresses. The sampling frequency was set at 256kHz for all tested frequencies and spatial resolution of sampling was set at 6 by 130 scan points in the height and length directions respectively, shown in Figure 4. This spatial resolution was found to be sufficient to capture both types of waves at the highest frequency, with greater scan densities having no significant effect on the measured signal.

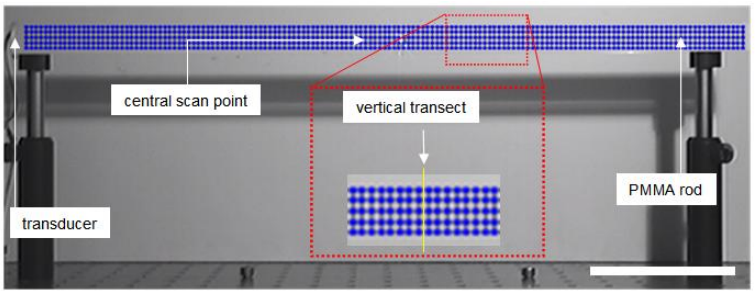

Figure 4 - Vibrometry scan area. Scan points on bar (shown in blue), support posts and transducer. Highlighted section shows location of vertical transect. Scale bar: 10cm.

5 Experimental Results

5.1 Mechanical excitation

The quality of the input signal delivered by the piezo transducer was evaluated by comparing input electrical signal with actual motion of the transducer. The latter was measured using the LVD workstation (Figure 5.)

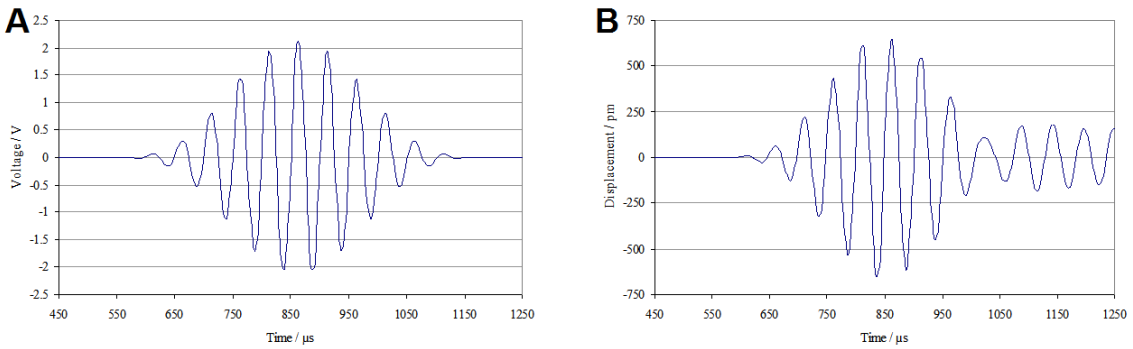

Figure 5 - Transducer input and response. A: transducer input signal, 20 kHz B: vibration output measured at center of piezo element.

As seen from Figure 5-B there is some residual vibration of the transducer even after the voltage has dropped to zero, as expected for piezo transducers [21]. The transducer vibration shapes were seen to be almost identical at each of the tested frequencies, the 10kHz deflection shape of the transducer and free end of the bar are shown Figure 6.

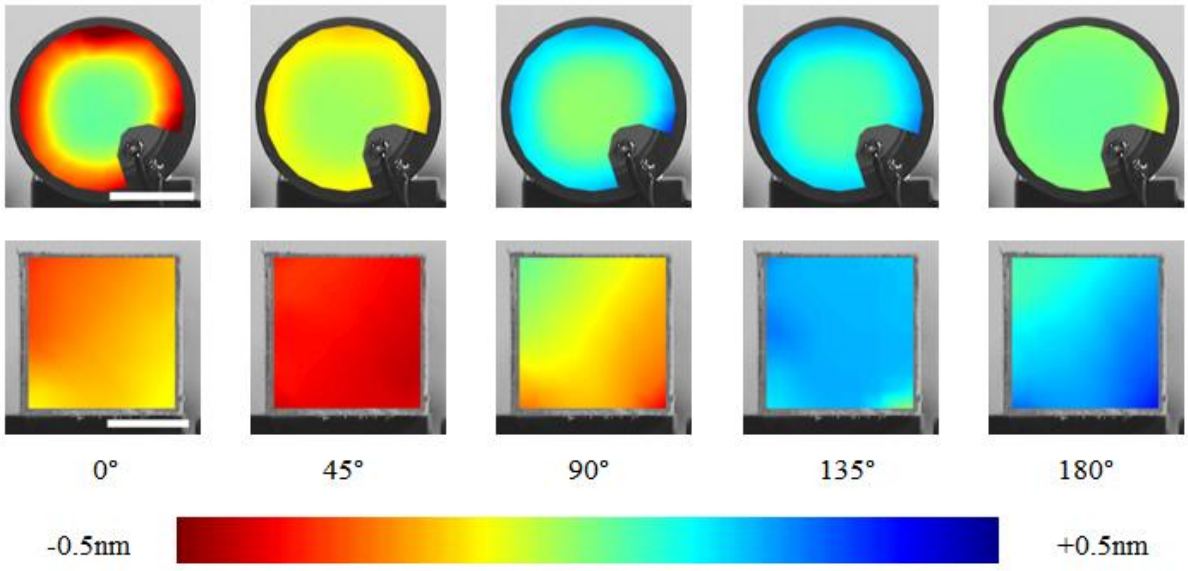

Figure 6 - Displacement shapes of transducer and free-end of PMMA bar at various phase angles during the excitation. Scale bar in 0° figure: 10mm.

The phases of the displacement of the bar's free end face were observed to be very uniform, as shown by the similar colours across the free end. This is evidence that by the time the compression wave reaches the free end, it had a plane wave front.

A further verification was carried out by measuring the velocity magnitude at different times using a vertical transect (shown in Figure 4), (Figure 7). Notably, the expected slight heterogeneity in vibration velocity across the wave front can be observed.

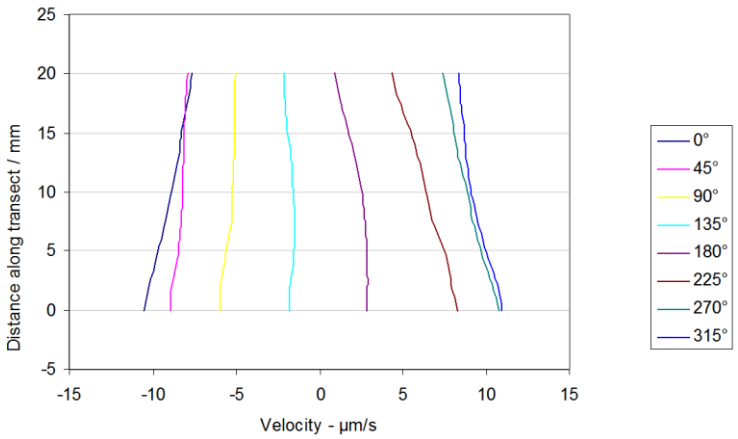

Figure 7 - Velocity magnitude (which is proportional to the stress/strain magnitude within the material, see Eq's 3-5) across vertical transect at different times for 20kHz signal. Small relative differences in magnitude indicate a flat wave front passing through the bar.

As such, the assumption can be justified that the propagating wave and therefore the resulting stresses are almost entirely σ_{11} stresses (as defined in Figure 2). However, the measured stress, denoted σ_{11*} here, will contain $\sigma_{11,}$ σ_{12} and σ_{13} stresses that are inseparable along the integration line of the laser. Using the finite element analysis (FEA) model, the calculated contribution of each of these stresses shows that σ_{12} and σ_{13} stresses are negligible (<0.1%) compared to σ_{11} .

The presented method relies upon the waves propagating through the bar as plane waves, as demonstrated in Figure 7. Should the propagating wave front encounter regions of non-planar stress/strain there will be errors associated with the use of Eq 5.

5.2 Sensitivity

The high sensitivity of the laser Doppler technique allows for an unprecedented sensitivity in measuring the internal strains within the PMMA bar. To estimate the lowest observable strains the 20kHz input signal was attenuated in 10dB steps until the signal was no longer visible against background noise. At high attenuations however the number of averages needed to register a signal rose to 2k. The lowest observable strain (estimated from Eq 5) was measured to be in the range of $1x10^{-11}$. Offering a sensitivity 5 orders of magnitude higher than traditional strain gages. This figure may not constitute the lowest limit possible using Doppler interferometry as it is based on Eq 5, and is therefore material/sample and vibrometer specific. Placing the length scales into perspective, this strain measurement is equivalent to observing a reduction in the earth's diameter by approximately 0.1mm.

5.3 Stress estimation

By working in the time domain, the time evolution of mechanical stress at any point within the scan area could be quantified (one point representing the average along one line of integration). As an example, the time-resolved stress fluctuations of the central scan point is shown in Figure 4, for an

excitation frequency of 20kHz. Using Eq 5, a documented Young's modulus of 3.6GPa and refractive index of 1.485 [10]), stress fluctuations are quantified in response to single wave packet (starting at t<1400μs). Remarkably the second wave packet detected (visible at t>1500μs) results from the reflection of the first packet from the free end of the bar.

It should be noted that as the angle of incidence of the laser beam on the PMMA surface varied between 0° and 14° due to the divergent scanning lines from the scanning LDV, there is a change in the optical length through the bar (from 20.0mm to 20.6mm) that was not incorporated into the calculation of the internal stress. This correction factor however can be incorporated into the calculations if the geometric configuration are known, and should be taken into consideration for the more demanding tomographic reconstructions of the 3D structure of the stress field.

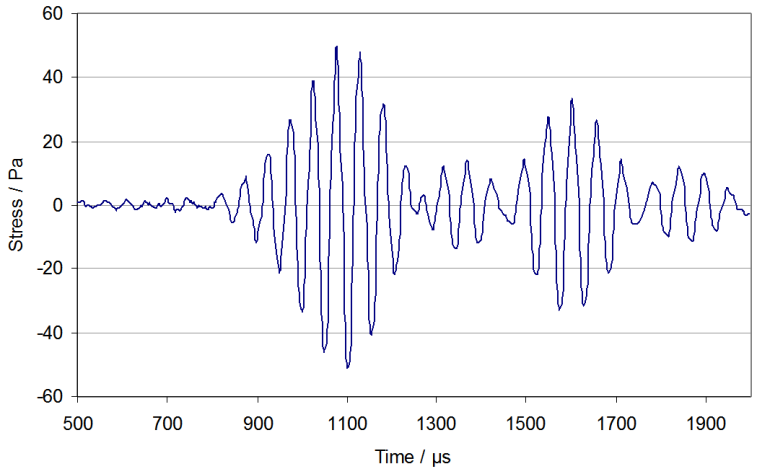

Figure 8 - σ_{11^*} evolution of central scan point.

The time evolution of the longitudinal waves over the whole scan area for 20kHz is shown in Figure 9.

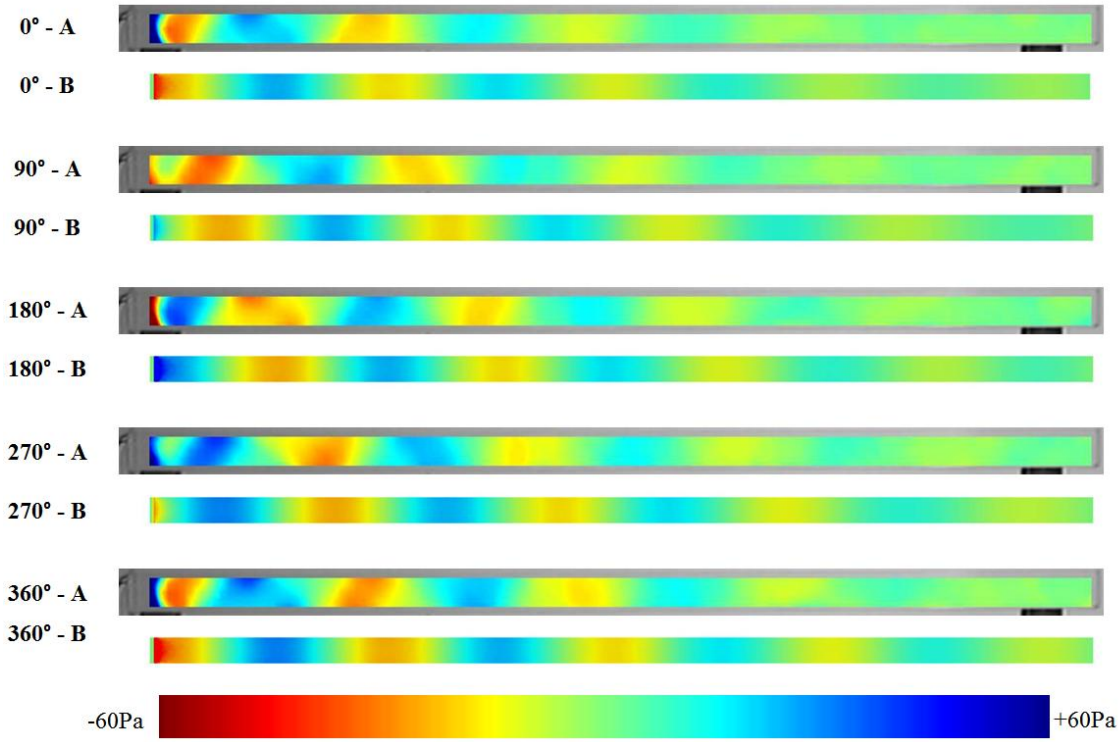

Figure 9 - Quantified time evolution of longitudinal σ_{11*} stress wave at 20kHz. A: Experimental value. B: FEA value.

6 Finite element analysis

In order to assess the accuracy of the method we employ 3D linear time-dependant FEA of the PMMA bar and a thin metal disc acting as the force transducer. As with the experimental work the time evolution of stress values within the solid are analysed.

6.1 Model details

The bar and transducer were modelled as linear elastic with tetrahedral elements of quadratic order used throughout. A mesh and time increment sensitivity study were conducted until solution convergence was achieved. This configuration corresponded to an element size of approximately $\lambda/20$ and a time step of T/20, where λ and T are respectively the wavelength and period of the elastic wave in the PMMA. The Young's modulus used was 3.6GPa (assuming a Poisson's ratio and density of 0.3 and 1,100kgm^{-3} respectively). The transducer at the end of the bar was given a time dependant velocity similar to the real signal seen in Figure 5. The magnitude of the transducer velocity, and thus force imparted to the bar, was approximated by matching the model value with the observed surface Rayleigh wave deflection. This was considered to be the best method of estimating the input force magnitude as it would be independent of bulk motion in the direction of the longitudinal wave propagation due to inertial forces. Once experimental and model surface deflection values were in close agreement the effective force magnitude was known, and peak values estimated to be 0.12N.

6.2 Time evolution of longitudinal wave

A comparison between experimentally derived and FEA stress values, the time resolved stress of a single measurement point (at 20kHz excitation) is shown in Figure 10. There is good agreement in both magnitude and phase. A number of factors can be identified that can contribute to some discrepancies between experimental data and FEA. The exact values of material properties of PMMA bar, especially Young's modulus, can vary from specifications and even along the material. The exact geometry of the PMMA bar can deviate from a perfect parallelogram. Although less likely, some mild non-linear elastic effects and damping may occur that are not captured by the FEA model used here.

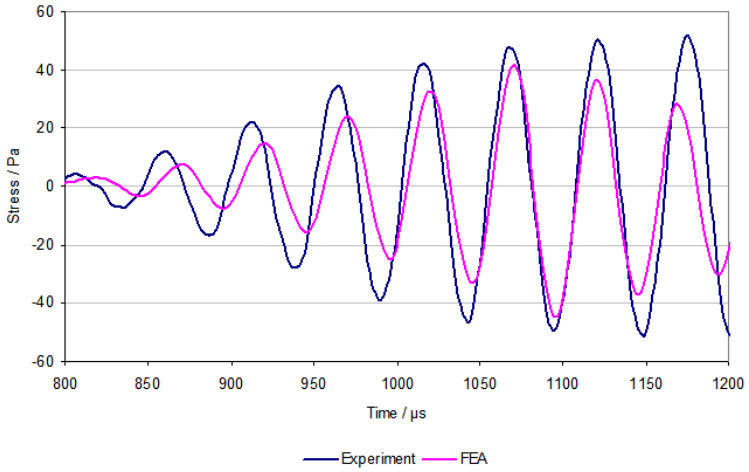

Figure 10 – Time-resolved stress fluctuations at single point in PMMA bar.

The FEA calculated mid-plane σ_{11} stress at 20kHz is shown in Figure 9. There is very good agreement with not only the magnitude (Figure 10), but also with stress distribution along the bar (Figure 9). For the same point depicted in Figure 10, the peak magnitudes of the σ_{12} and σ_{13} stresses are approximately 0.1% of σ_{11}. We conclude therefore that the approximation $\sigma_{11*} \approx \sigma_{11}$ is acceptable in these experimental conditions.

7 Conclusions

Using the established relationship between elastic strain and refractive index, we provide the demonstration that LDV measurements can yield a temporally and spatially accurate quantification of stress within a solid. In the present experimental sample, a PMMA bar, actuation of one end gives rise to two concurrent elastic waves, longitudinal and Rayleigh surface waves. These two wave types can be measured independently by exploiting different measurement principles of LDV. The method also enables time-resolved visualisation of internal longitudinal waves.

We readily point out however that the magnitude of the estimated stress cannot simply be decoupled into contributory stresses. While we assume a single stress, σ_{11*}, other stresses will contribute. The FEA suggest however that for this load scenario the other stresses are insignificant in magnitude, and

we can have some confidence in assuming that the measured σ_{11*} stress is an accurate measure of the true σ_{11} stress.

The presented study aims at stimulating interest in this practical and powerful investigative technique into the stresses within transparent media. While a direct comparison with contact strain gauge measurements is practical, its scope is limited. This is because the strains reported here are several orders of magnitude lower than those reported with conventional strain gauges. Strains as low as $1x10^{-11}$ could be measured, a sensitivity which exceeds those previously reported in the literature.

Acknowledgements:

The authors would like to kindly thank the Biotechnology and Biological Sciences Research Council (BBSRC) for funding. D. Robert is supported by the Royal Society of London and the Wolfson Foundation.

8 References

[1] R. D. Mindlin, "A Review of the Photoelastic Method of Stress Analysis. II," *Journal of Applied Physics*, vol. 10, no. 5, p. 273, 1939.

[2] P. A. Chinnery, "The schlieren image of two-dimensional ultrasonic fields and cavity resonances," *The Journal of the Acoustical Society of America*, vol. 101, no. 1, pp. 250–256, Jan. 1997.

[3] A. J. Allen, M. T. Hutchings, C. G. Windsor, and C. Andreani, "Neutron diffraction methods for the study of residual stress fields," *Advances in Physics*, vol. 34, no. 4, pp. 445–473, Jan. 1985.

[4] C. Matteï, X. Jia, and G. Quentin, "Direct experimental investigations of acoustic modes guided by a solid–solid interface using optical interferometry," *The Journal of the Acoustical Society of America*, vol. 102, no. 3, pp. 1532–1539, Sep. 1997.

[5] X. Jia, C. Matteï, and G. Quentin, "Analysis of optical interferometric measurements of guided acoustic waves in transparent solid media," *Journal of Applied Physics*, vol. 77, no. 11, p. 5528, 1995.

[6] R. Longo, S. Vanlanduit, and P. Guillaume, "Material properties identification using ultrasonic waves and laser Doppler vibrometer measurements: a multi-input multi-output approach," *Measurement Science and Technology*, vol. 24, no. 10, p. 105206, Oct. 2013.

[7] R. Wimberger-Friedl, "The assessment of orientation, stress and density distributions in injection-molded amorphous polymers by optical techniques," *Progress in Polymer Science*, vol. 20, no. 3, pp. 369–401, 1995.

[8] R. M. Waxler and W. C. E, "Effect of Hydrostatic Pressure on the Refractive Indices of Some Solids," *Journal of Research of the National Bureau of Standards -A*, vol. 69A, no. 4, pp. 325–333, 1965.

[9] E. D. D. Schmidt and K. Vedam, “Variation of the refractive indices of CaF2, BaF2 and β-PbF2 with pressure to 7 kb,” *Journal of Physics and Chemistry of Solids*, vol. 27, no. 10, pp. 1563–1566, Oct. 1966.

[10] D. V. Nazarov, A. L. Mikhailov, A. V. Fedorov, S. F. Manachkin, V. D. Urlin, A. V. Men’shikh, S. A. Finyushin, V. A. Davydov, and E. V. Filinov, “Properties of optically transparent materials under quasi-entropic compression,” *Combustion, Explosion, and Shock Waves*, vol. 42, no. 3, pp. 351–355, May 2006.

[11] K. Nakamura, M. Hirayama, and S. Ueha, “Measurements of air-borne ultrasound by detecting the modulation in optical refractive index of air,” in *IEEE Ultrasonics Symposium*, 2002, pp. 609–612.

[12] K. Nakamura, “Sound field measurement through the acousto-optic effect of air by using laser Doppler velocimeter,” in *4th Pacific Rim Conference on Lasers and Electro-Optics*, 2001, vol. 1, pp. 154–155.

[13] A. Torras-Rosell, S. Barrera-Figueroa, and F. Jacobsen, “Sound field reconstruction using acousto-optic tomography.,” *The Journal of the Acoustical Society of America*, vol. 131, no. 5, pp. 3786–93, May 2012.

[14] E. Olsson, “Three-dimensional selective imaging of sound sources,” *Optical Engineering*, vol. 48, no. 3, p. 035801, Mar. 2009.

[15] A. Dittmar and R. Behrendt, “Measuring the 3D propagation of sound waves using scanning laser vibrometry,” in *Berlin Beamforming Conference*, 2008.

[16] Y. Oikawa, “Sound Field Measurements Based on Reconstruction from Laser Projections,” in *IEEE International Conference on Acoustics, Speech, and Signal Processing*, 2005, vol. 4, pp. 661–664.

[17] C. Vuye, S. Vanlanduit, and P. Guillaume, “Accurate estimation of normal incidence absorption coefficients with confidence intervals using a scanning laser Doppler vibrometer,” *Optics and Lasers in Engineering*, vol. 47, no. 6, pp. 644–650, Jun. 2009.

[18] L. Zipser, H.-D. Seelig, and H. Franke, “Refracto-vibrometry for visualizing ultrasound in small-sized channels, cavities and objects,” in *International Ultrasonics Symposium*, 2009, pp. 2588–2591.

[19] E. Olsson and K. Tatar, “Sound field determination and projection effects using laser vibrometry,” *Measurement Science and Technology*, vol. 17, no. 10, pp. 2843–2851, Oct. 2006.

[20] E. Olsson, “Selective imaging of sound sources in air using phase-calibrated multiwavelength digital holographic reconstructions,” *Optical Engineering*, vol. 46, no. 7, p. 075801, Jul. 2007.

[21] L. Zipser, F. Wachter, and J.-U. Wustling, “Generation of solitary acoustic impulses,” in *1996 IEEE Ultrasonics Symposium. Proceedings*, vol. 1, pp. 555–558.